Improper Coordination of BamA and BamD Results in Bam Complex Jamming by a Lipoprotein Substrate

Muralidhar Tata,[a] Anna Konovalova[a]

[a]Department of Microbiology and Molecular Genetics, McGovern Medical School, The University of Texas Health Science Center at Houston (UTHealth), Houston, Texas, USA

ABSTRACT The β-barrel assembly machinery, the Bam complex, is central to the biogenesis of integral outer membrane proteins (OMPs) as well as OMP-dependent surface-exposed lipoproteins, such as regulator of capsule synthesis protein F (RcsF). Previous genetic analysis established the model that nonessential components BamE and BamB have overlapping, redundant functions to enhance the kinetics of the highly conserved BamA/BamD core. Here we report that BamE plays a specialized nonredundant role in the Bam complex required for surface exposure of RcsF. We show that the lack of *bamE*, but not *bamB*, completely abolishes assembly of RcsF/OMP complexes and establish that the inability to assemble RcsF/OMP complexes is a molecular reason underlying all synthetic lethal interactions of $\Delta bamE$. Our genetic analysis and biochemical cross-linking suggest that RcsF accumulates on BamA when BamA cannot engage with BamD because of its limited availability or the incompatible conformation. The role of BamE is to promote proper coordination of RcsF-bound BamA with BamD to complete OMP assembly around RcsF. We show that in the absence of BamE, RcsF is stalled on BamA, thus blocking its function, and we identify the lipoprotein RcsF as a bona fide jamming substrate of the Bam complex.

IMPORTANCE The β-barrel assembly machinery, the Bam complex, consists of five components, BamA to -E, among which BamA and BamD are highly conserved and essential. The nonessential components are believed to play redundant roles simply by improving the rate of β-barrel folding. Here we show that BamE contributes a specific and nonoverlapping function to the Bam complex. BamE coordinates BamA and BamD to form a complex between the lipoprotein RcsF and its partner outer membrane β-barrel protein, allowing RcsF to reach the cell surface. In the absence of BamE, RcsF accumulates on BamA, thus blocking the activity of the Bam complex. As the Bam complex is a major antibiotic target in Gram-negative bacteria, the discovery that a lipoprotein can act as a jamming substrate may open the door for development of novel Bam complex inhibitors.

KEYWORDS Gram-negative envelope biogenesis, Rcs phosphorelay, surface-exposed lipoproteins

The heteropentameric β-barrel assembly machinery, the Bam complex, plays a central role in the outer membrane (OM) biogenesis in Gram-negative bacteria by promoting folding and insertion of integral β-barrel OM proteins (OMPs) (1). Although the overall function of the Bam complex is well established, the mechanistic contribution of its individual components (BamA to -E) is not well understood. BamA and BamD have emerged as the core components because of their essential nature and the high degree of conservation (2, 3). Genetic and biochemical evidence suggests that BamD recruits incoming OMP substrates (4, 5), while BamA is considered central for OMP folding/membrane integration due to its transmembrane nature (3, 6). The function of

BamB, -E, and -C remains elusive. These components are not essential and are conserved in some, but not all, Gram-negative bacteria (7); therefore, they are unlikely to contribute a fundamental function to OMP assembly and are viewed as accessory components to enhance the kinetics of the BamAD core. Several lines of evidence support this model. Null mutations in *bamB* affect assembly of high-volume OMP substrates, such as porins, but do not affect the assembly of less abundant, and often more complex OMPs, including LptD and TolC (8–10). BamB is required for full efficiency of OMP assembly *in vitro* (11–13). Deletions of *bamE* and *bamC* do not affect the assembly of any single OMP; the most notable phenotype of *bamE* is its synthetic lethality at the physiological temperature (37°C) when combined with other *bam* mutations, including *bamB* (14–16). The *bamE bamB* double mutant can only grow either when the demand for the Bam complex efficiency is lowered under conditions of slow growth (minimal medium at 30°C) (15) or when the highly active σE stress response minimizes the periplasmic accumulation of toxic unfolded OMP substrates (17, 18). This observation led to the idea that BamE and BamB have overlapping, redundant functions supporting high efficiency of the OMP assembly under conditions of rapid growth (15).

In pursuit of the molecular mechanism of signal transduction by the Rcs stress response, we discovered that the *Escherichia coli* OM lipoprotein RcsF adopts a transmembrane topology by spanning the lumen of OMPs, most commonly OmpA (19). The N-terminal surface-exposed domain of RcsF is anchored in the outer leaflet of the OM by a lipid moiety to monitor disruptions in LPS packing (19, 20). Once stress is detected, the signal is transduced via the lumen of an OMP to the periplasmic C-terminal folded domain of RcsF to activate downstream signaling (20), releasing IgaA inhibition of the RcsCDB phosphorelay (21, 22). In response, RcsB acts as a homodimer or as a heterodimer with RcsA to regulate gene expression and promote envelope adaptation to stress (22).

Using a combination of *in vitro* and *in vivo* approaches, we previously demonstrated that the OMP barrel is folded around RcsF and that this reaction is catalyzed by the Bam complex *in vivo*. We thus uncovered a novel function of the Bam complex in the biogenesis of surface-exposed lipoproteins (19). We also showed that a *bamE* deletion completely abolishes assembly of RcsF/OMP complexes (20). Therefore, the RcsF/OMP complex is the first-described substrate of the Bam complex that requires BamE activity, suggesting that specialized activities of the Bam complex are needed for the assembly of this more challenging substrate. In the present study, we used the RcsF/OMP assembly as a tool to probe BamE function. Using genetic analysis and biochemical cross-linking, we demonstrate that RcsF is recruited to the Bam complex via BamA and that BamE plays a specialized, nonredundant role in coordinating lipoprotein/BamA and OMP/BamD core components to complete RcsF/OMP assembly. In the absence of BamE, RcsF accumulates on BamA, reducing the functional pool of Bam complexes in the cell. Δ*rcsF* is a potent suppressor of all *bamE* synthetic lethal interactions, restoring growth and OMP assembly in the otherwise lethal *bamE* double mutant backgrounds. Therefore, the lipoprotein RcsF represents a jamming substrate of the Bam complex.

RESULTS

RcsF inhibits the function of the Bam complex in the Δ*bamE* background. We previously reported that BamE is required for assembly of RcsF/OMP complexes. In the Δ*bamE* strain, the reduction of RcsF/OMP cross-linking (estimated molecular weight of 50 kDa) is accompanied by the increase of RcsF/BamA cross-linking (estimated molecular weight of 110 kDa) (Fig. 1), suggesting that RcsF is arrested on BamA when the complex assembly is blocked. Here we began to elucidate the consequence of RcsF arrest on Bam complex function. We observed that around 30% of BamA is sequestered with RcsF in the Δ*bamE* strain as judged by the formaldehyde cross-linking (Fig. 1 and 2); however, this fraction is likely to be higher because cross-linking is not performed to saturation. Although this fraction is not sufficient to cause an obvious OMP assembly defect in the Δ*bamE* mutant, we reasoned that strains with lower levels or activity of
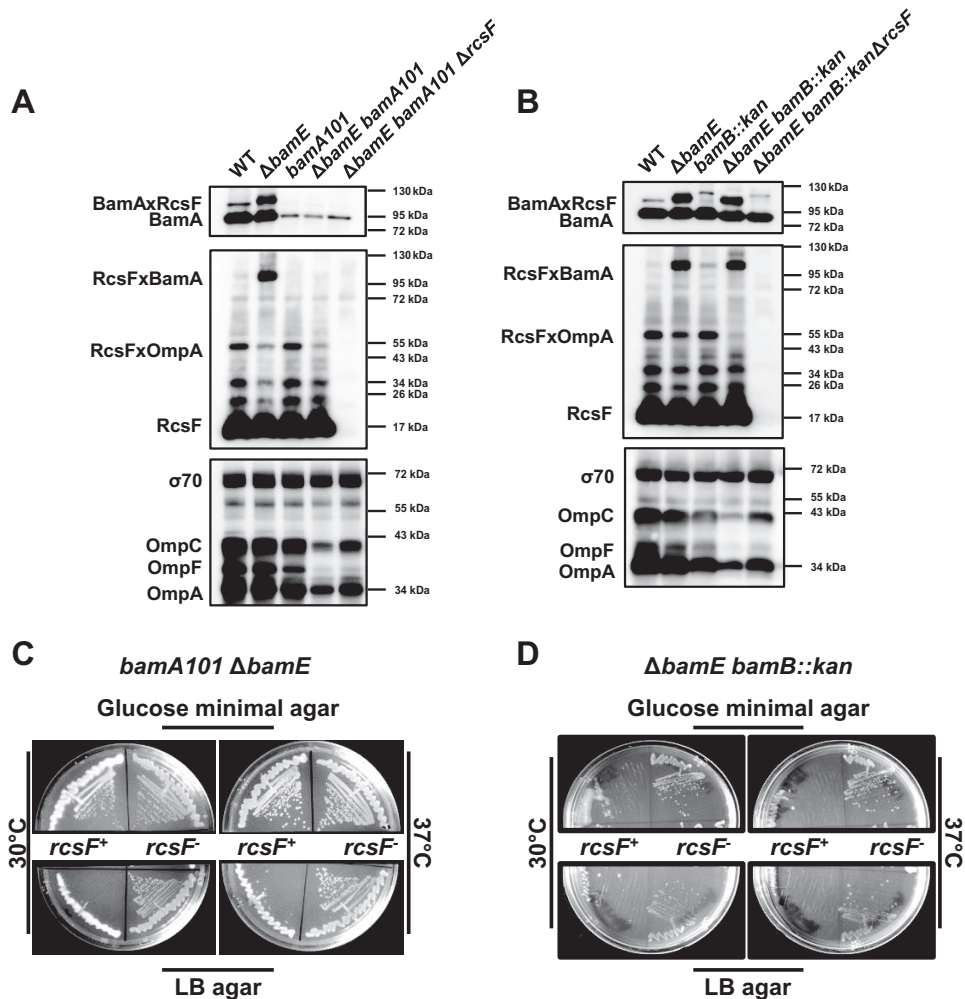
FIG 1 BamE plays a specific nonredundant role in the Bam complex required for the RcsF/OMP assembly. Δ*bamE* and not *bamA101* (A) or *bamB*::Kan (B) mutations result in the significant decrease of RcsF/OMP cross-linking. Δ*rcsF* improves OMP assembly in the corresponding double mutants (A and B, lower panels). Strains were grown in glucose minimal medium at 30°C, subjected to formaldehyde cross-linking, and analyzed by immunoblotting using anti-RcsF and anti-BamA antibodies. Immunoblot analysis of the total OMPs and σ70 (loading control) levels was performed on the total cell extracts (without cross-linking). Plate growth phenotype of *bamA101* Δ*bamE* (C) and Δ*bamE bamB*::Kan (D) double mutants and their Δ*rcsF* derivatives. Strains were streaked on indicated agar plates; plates were incubated at 30°C or 37°C. Growth was assayed after 48 h.

BamA would be more sensitive to RcsF-dependent BamA sequestration, which may explain the well-documented conditional synthetic lethality of Δ*bamE* when combined with *bamA101* or *bamB* mutations (14, 15). The *bamA101* mutation harbors a Tn5 insertion in the promoter region of *bamA*, decreasing BamA levels approximately 10-fold (23). Unlike the *bamA101* mutation, a *bamB* mutation does not affect BamA levels but confers a general OMP assembly defect due to partially compromised Bam complex activity (10). Accordingly, the *bamB* strain also cannot tolerate a further reduction in BamA level or activity, and *bamB* is essential in the *bamA101* background at temperatures above 24°C (Table 1).

To test our hypothesis, we first constructed Δ*bamE bamA101* and Δ*bamE bamB* double mutants with or without Δ*rcsF* under permissive condition (glucose minimal medium at 30°C) and tested these mutants for RcsF/OMP assembly. Unlike Δ*bamE*, neither *bamA101* nor *bamB* affected RcsF/OMP assembly (Fig. 1A and B), demonstrating a specific role of BamE in this process. As expected, the introduction of Δ*bamE* into either the *bamA101* or *bamB* background resulted in a significant reduction of RcsF/OMP cross-linking (Fig. 1A and B). The Δ*bamE bamB* strain largely phenocopied Δ*bamE*,
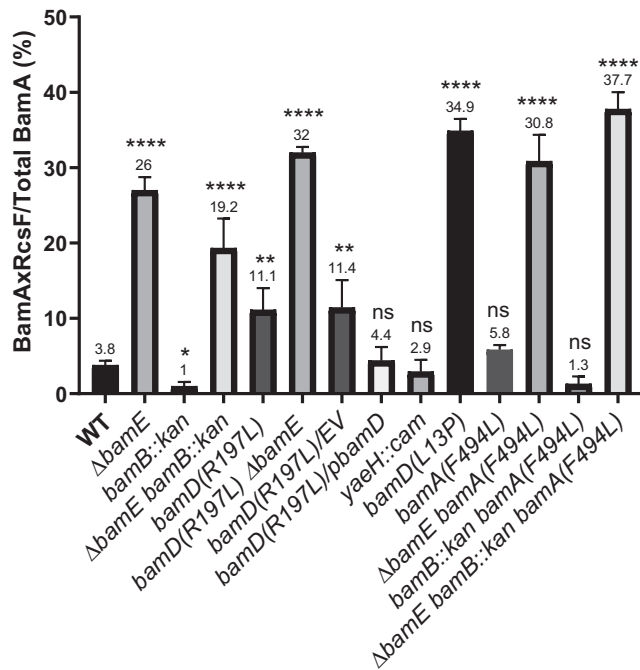
FIG 2 Quantitative analysis of the BamA fractions cross-linked to RcsF. Strains were grown and treated as described in the legend to Fig. 1. The intensity of BamA and BamAxRcsF bands was quantified using GelQuantNet software. Graphs represent mean fraction of BamAxRcsF as a percentage of total BamA ± standard error of the mean (SEM) based on at least three independent biological replicates. Significance analysis was performed using unpaired t test by comparing all strains with the WT. The asterisks represent $P < 0.0001$ (****), $P < 0.001$ (**), and $P < 0.02$ (*). For individual immunoblots, and their quantification, refer to Fig. S1 to S6 and Table S1.

and RcsF accumulated on BamA. We were not able to detect the RcsF/BamA cross-link in either of the *bamA101* strains, likely because BamA levels are significantly reduced (Fig. 1A and B).

According to our hypothesis, RcsF sequestration could reduce the functional pool of BamA to lethal levels in the double mutants. In strong support of this hypothesis, we determined that the temperature-sensitive phenotype of Δ*bamE bamA101* and Δ*bamE bamB* double mutants is *rcsF* dependent (Table 1; Fig. 1C and D). Δ*rcsF* restored growth of these double mutants on LB at 30°C and 37°C, although the Δ*bamE bamB* Δ*rcsF* strain grew slower than the wild type (WT) on LB agar at 37°C. Consistent with the growth phenotype, we also observed that the introduction of Δ*rcsF* improved OMP assembly in Δ*bamE bamA101* (Fig. 1A, compare the last two lanes) and Δ*bamE bamB* (Fig. 1B,

TABLE 1 Plate growth phenotype of the OMP assembly-defective double mutants[a]

| | Growth of strain in medium: | | | | | |
| | Glucose minimal medium | | | LB | | |
Mutation	Parent	Δ*rcsF*	Δ*rcsB*	Parent	Δ*rcsF*	Δ*rcsB*
Δ*bamE bamB*::Kan	TS@37	+	TS@37	TS@30	+	TS@30
Δ*bamE bamA101*	+	+	TS@30	TS@30	+	TS@30
bamA101 bamB8[b]	TS@30	TS@30	ND	−	−	ND
degP::Cm *bamB*::Kan	+	+	ND	TS@37	TS@37	ND
bamE::Cm *bamD*(R197L)	+	+	ND	TS@37	+	ND

[a]The strains were assayed for the ability to grow and form isolated colonies on top of the solid agar plates at 24°C, 30°C, and 37°C. The temperature-sensitive (TS) phenotype is indicated by the lowest temperature (°C) at which growth was no longer observed. The + and − signs indicate growth or lack of growth, respectively, at all temperatures tested; ND, not determined.

[b]*bamB8* is a markerless null allele of *bamB* (46). It was used to assay *bamA101* interaction due to the incompatible antibiotic resistance marker of *bamB*::Kan.

compare the last two lanes) double mutants, although it was not restored to the WT levels.

Growth under low temperatures and on minimal glucose medium leads to increased Rcs activity evident by the mucoid phenotype. This phenomenon is poorly understood but is explained at least in part by the increased levels of RcsA (22). Because Rcs activity can be toxic (21, 24) and Δ*rcsF* inactivates the pathway, we tested whether inactivation of Rcs by Δ*rcsB* would also suppress Δ*bamE bamA101* and Δ*bamE bamB* double mutants. We found that unlike Δ*rcsF*, Δ*rcsB* could not restore growth on LB; moreover, Δ*rcsB* resulted in more severe growth defects in the double mutants (Table 1). This result demonstrates that the suppression by Δ*rcsF* is independent of RcsF signaling function. Finally, the Δ*rcsF* mutation is not a general suppressor of OMP assembly mutants, because it is unable to suppress the *bamA101 bamB* and *bamB degP* (10) synthetic lethal pairs (Table 1).

Based on the above results, we concluded that the inability to assemble RcsF causes the conditional essentiality of *bamE*. In the absence of *bamE*, RcsF remains on BamA, sequestering BamA from functioning in the OMP assembly.

Proper engagement of BamA and BamD is critical for RcsF/OMP assembly. The Δ*bamE* mutant also displays a synthetic lethal interaction with *bamD(R197L)* (25). *bamD(R197L)* is a gain-of-function mutation which enables BamD to function independently of the direct interaction with BamA. It was isolated as a suppressor of the lethal *bamA(E373K)* mutation that targets a salt bridge critical for BamA-BamD coordination (26, 27). However, the *bamE bamD(R197L)* synthetic lethal pair is distinct from those described above, because *bamD(R197L)* does not confer any detectable phenotype in an otherwise WT background (25, 27). This intriguing synthetic lethality led to a proposed conformational cycling model, in which both *bamE* and *bamD(R197L)* bias BamA toward a distinct conformation, preventing it from undergoing the normal dynamic cycle needed for efficient OMP assembly (25).

Deletion of Δ*rcsF* restored growth of the *bamE*::Cm *bamD(R197L)* double mutant on LB at 37°C (Table 1), demonstrating that Δ*rcsF* acts as a *bamE* suppressor and suppresses all *bamE* synthetic lethal combinations regardless of the underlying defect. Surprisingly, however, the cross-linking experiments revealed that the *bamD(R197L)* mutation also led to increased RcsF accumulation on BamA, although the phenotype was milder than that observed for the *bamE* mutant (Fig. 2 and 3A).

We next sought to investigate the underlying reason for the phenotype of the *bamD(R197L)* strain. We envisioned two possible scenarios by which the *R197L* mutation could affect the RcsF/OMP assembly. In the first scenario, R197L would bias BamD toward a conformation unable to engage with RcsF-bound BamA. In the second scenario, BamD(R197L) would engage with RcsF-bound BamA in an unproductive manner, arresting the RcsF/OMP assembly process. We used genetic analysis to differentiate between these scenarios. *bamD(R197L)* is expected to be recessive to the WT *bamD* allele in the former case, while in the latter case it would confer a dominant negative phenotype. To test for dominance, we introduced the WT copy of *bamD* on a low-copy-number pZS21 plasmid into the *bamD(R197L)* strain and performed biochemical cross-linking experiments (Fig. 3B). RcsF/BamA cross-linking was reduced back to the WT levels in the *bamD* merodiploid strain compared with the elevated levels in the empty vector (EV) control (Fig. 2 and 3B). This recessive nature of the *bamD(R197L)* mutation is indicative of its loss-of-function nature regarding RcsF/OMP assembly, which is in stark contrast to its gain-of-function nature for general OMP assembly (25, 26).

We next reasoned that if the inability of BamD(R197L) to engage with RcsF-bound BamA resulted in RcsF stalling on BamA, then the same phenotype would be observed when BamD was absent. Like *bamA*, *bamD* is essential (2), so we used *bamD(L13P)*, a mutation in the signal sequence that causes inefficient export of BamD across the Sec translocon, resulting in an approximately 10-fold reduction in BamD levels (Fig. 3C) (8). Importantly, the mature BamD protein still has the WT sequence in this case. Like
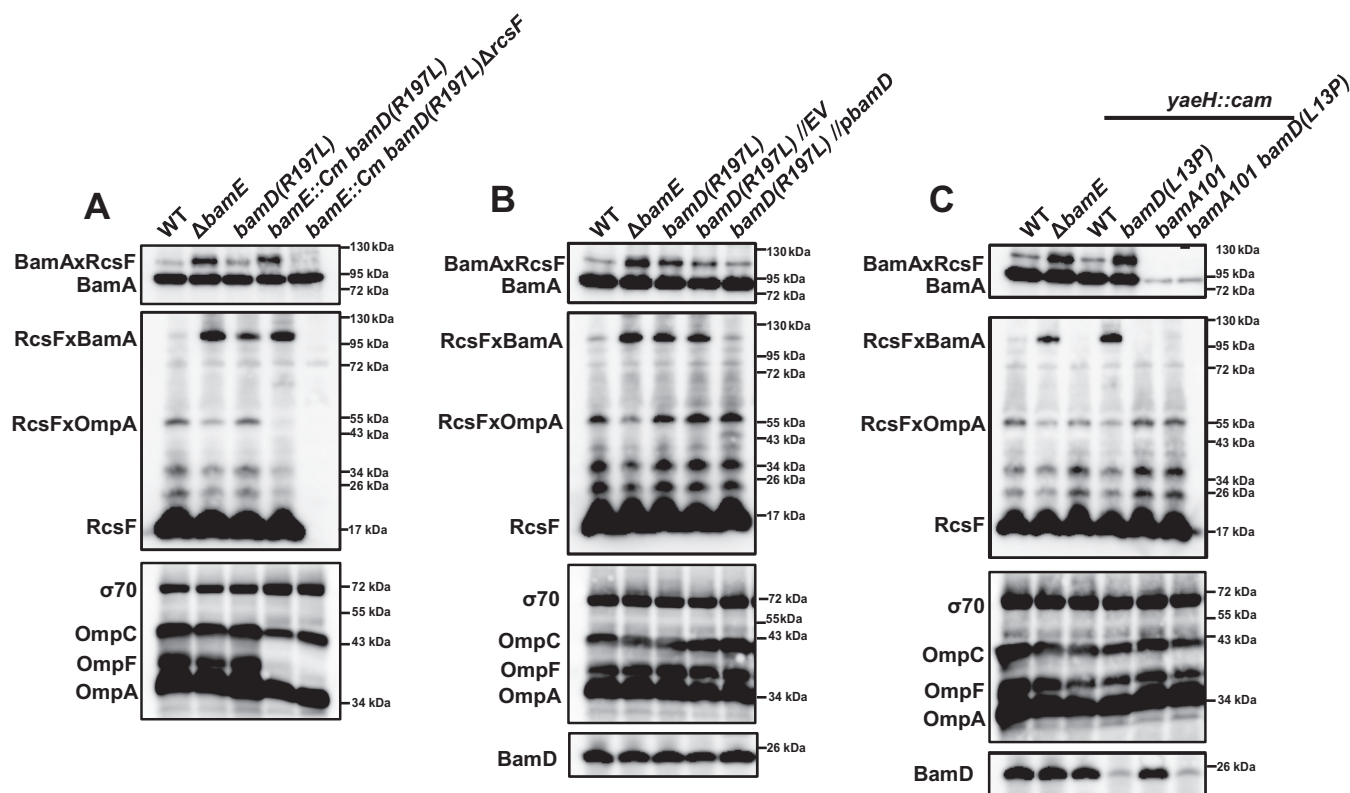
FIG 3 Improper coordination of BamA and BamD results in RcsF accumulation on BamA. (A) *bamD*(R197L) results in increased RcsF/BamA cross-linking. (B) The *bamD*(R197L) mutation is recessive to the WT *bamD* allele. (C) Decreased levels of BamD relative to BamA abolish RcsF/OMP assembly, leading to RcsF accumulation on BamA. Strains were grown in glucose minimal medium at 30°C, subjected to formaldehyde cross-linking, and analyzed by immunoblotting using anti-RcsF and anti-BamA antibodies. Immunoblot analysis of the total OMPs and σ70 (loading control) levels was performed on the total cell extracts (without cross-linking).

bamA101, *bamD*(L13P) affects the efficiency of the OMP assembly by an overall reduction in the number of functional Bam complexes (8). However, *bamD*(L13P) results in a phenotype distinct from *bamA101*, as no RcsF/OMP complexes were formed and RcsF accumulated on BamA (Fig. 2 and 3C). Importantly, the *bamA101 bamD*(L13P) double mutant, in which the ratio of BamA and BamD is restored, showed restoration of RcsF/OMP assembly (Fig. 2 and 3C). Based on these results, we concluded that RcsF accumulates on BamA when BamA cannot engage with BamD either because of its limited availability [e.g., *bamD*(L13P)] or because BamD is in an incompatible conformation [e.g., *bamD*(R197L)]. Because both of the *bamD* mutant strains phenocopied ΔbamE, we concluded that the underlying defect of ΔbamE is also related to BamA/BamD engagement.

Several *bamA* suppressors that enable growth of the ΔbamE bamB strain under nonpermissive conditions have been previously isolated (15). One such mutation, *bamA*(F494L), is of particular interest. It is a gain-of-function mutation that also allows the cell to survive despite very low levels of BamD (28). This mutation also was independently isolated as a suppressor restoring the assembly of a defective OMP substrate, LptD(Y721D), which accumulates on BamD as a result of defective BamA/BamD coordination (4). We tested the effect of the *bamA*(F494L) mutation on RcsF cross-linking in single and double mutants (Fig. 4). We observed that *bamA*(F494L) did not change the RcsF cross-linking pattern in either of the strains, demonstrating that *bamA*(F494L) improves the OMP assembly defect without restoring RcsF/OMP assembly (Fig. 2 and 4).

DISCUSSION

The RcsF/OMP complex is a novel type of Bam-dependent protein complex consisting of a lipoprotein and an OMP partner. In this complex, an OMP barrel is folded
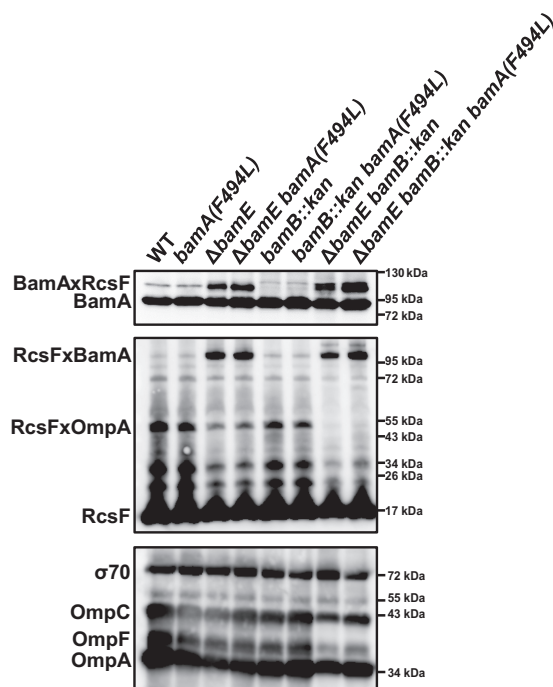
FIG 4 The *bamA*(*F494L*) mutation does not restore the RcsF/OMP assembly in the Δ*bamE bamB* strain. Strains were grown in glucose minimal medium at 30°C, subjected to formaldehyde cross-linking, and analyzed by immunoblotting using anti-RcsF and anti-BamA antibodies. Immunoblot analysis of the total OMPs and σ70 (loading control) levels was performed on the total cell extracts (without cross-linking).

around the RcsF unstructured region, allowing it to adopt a transmembrane topology with its lipidated N-terminal domain exposed on the cell surface (19). Assembly of this complex requires some of the distinct activities of the Bam machinery, specifically, the ability to (i) simultaneously recognize both lipoprotein and OMP substrates, (ii) translocate the RcsF lipid moiety to the OM outer leaflet, and (iii) coordinate lipoprotein surface exposure with OMP assembly. Previous studies established that OMP substrates are recruited to the Bam complex via BamD (4, 5). Here we show that RcsF is recruited via BamA and independently of BamD. The progression of RcsF/OMP assembly requires BamE, which plays a specific role in coordinating RcsF-bound BamA with BamD. In the absence of BamE, RcsF remains stalled on BamA, preventing BamA from functioning in the OMP assembly, and thereby acting as a jamming substrate of the Bam complex.

BamE is not essential, and its function in the Bam complex is poorly studied, primarily due to the lack of a significant phenotype of Δ*bamE* in OMP assembly (14, 16). The most notable phenotype is the well-documented synthetic lethal interactions when Δ*bamE* is combined with other *bam* mutations, including *bamB* (14, 15). This observation led to the idea that BamE and BamB have overlapping, redundant functions to enhance the kinetics of the BamAD core components (15). Here we show that, unlike what was previously thought, BamE plays a specific nonredundant role in the Bam complex. BamE, but not BamB, is critical for the RcsF/OMP assembly. Moreover, RcsF-dependent sequestration of BamA is the molecular reason underlying synthetic lethal interactions of Δ*bamE*, including that with *bamB*. Δ*rcsF* acts as a suppressor of growth and OMP assembly in the Δ*bamE bamB* and Δ*bamE bamA101* double mutants. In the accompanying paper (29), Hart et al. use a quantitative proteomic analysis to demonstrate that the *bamE bamB* double mutant displays a broad *rcsF*-dependent OMP assembly defect. Removal of *rcsF* results in the global restoration of OMP levels nearly to the same extent as the previously characterized *bamA*(*F494L*) suppressor (4, 15, 28). This proteomic analysis is consistent with general inhibition of the Bam complex function by stalled RcsF.

Based on the results presented above, we proposed that BamE plays a specific role

in RcsF/OMP assembly by promoting proper coordination of RcsF-bound BamA with BamD, likely bound to the OMP substrate. BamA/BamD coordination is essential for OMP assembly and cell growth. In WT cells, it involves conformational changes in BamA and BamD regulated through a direct interaction between the two proteins at the BamA Potra 5 domain interface (26, 27). bamD(R197L) is a gain-of-function mutation for OMP assembly, in which BamD is biased toward an altered conformation, bypassing the requirement for BamA-induced activation (26, 27). bamD(R197L) is compatible with both WT and otherwise-lethal E373K alleles of bamA (26, 27). In contrast, we showed that bamD(R197L) is a recessive, partial-loss-of-function mutation with regard to RcsF assembly, resulting in an increase in RcsF/BamA cross-linking, thus phenocopying the ΔbamE mutation. Importantly, the same phenotype is also observed under the conditions of BamD limitation in the bamD(L13P) strain, and therefore, we concluded that RcsF accumulates on BamA when BamA is not engaged with BamD.

BamE is clearly dispensable for BamA/BamD coordination during normal OMP assembly because it is not essential and does not confer an OMP assembly defect (14, 16). So why is BamE important for BamA/BamD coordination during RcsF/OMP assembly? We propose that RcsF binding to BamA alters BamA conformation in such a way that it is unable to directly engage with BamD and therefore requires BamE activity for this process. In the absence of BamE, BamA/BamD cannot communicate to complete OMP assembly around RcsF, and RcsF remains stalled on BamA. The RcsF-induced conformational change of BamA also causes incompatibility with BamD(R197L) regardless of the presence of BamE, which is reminiscent of the reciprocal genetic incompatibility of BamD(R197L) with BamA variants with an altered electrostatic network at the BamA-Potra 5/BamD interface (26). Based on the structure of the Bam complex, BamE interacts with both BamA and BamD (30, 31). More studies are needed to understand whether BamE coordinates BamA/BamD during RcsF/OMP assembly by regulating the conformation of BamA, BamD, or both.

Another two-partner lipoprotein/OMP complex in E. coli is LptE/LptD, which is an essential complex for LPS transport across the OM (32). BamE activity is not required for LptE/LptD assembly (14, 16). The fundamental difference between RcsF/OMP and LptE/LptD is the lipoprotein topology in the complex (19, 33–35). We think it is likely that a specific requirement for BamE in RcsF/OMP assembly is directly related to the ability of the Bam complex to translocate RcsF lipid moieties to the outer leaflet of the OM, leading to the surface exposure of the RcsF N-terminal domain.

Our studies of RcsF/OMP assembly led to the discovery of a novel function of the Bam complex in the biogenesis of surface-exposed lipoproteins. Deciphering the RcsF/OMP assembly pathway not only would be highly informative for a further mechanistic understanding of this versatile macromolecular machinery but might also open the doors for novel therapeutic development strategies. The Bam complex has emerged as a major antibiotic target due to its central and essential role in the biogenesis of the OM, the primary factor of intrinsic antibiotic resistance in Gram-negative bacteria (36–38). Previous studies have explored the possibility of using OMP-derived-peptides that mimic native OMP substrates to inhibit the Bam complex via BamD (5). However, both assembly-defective OMP substrates and OMP-derived peptides strongly activate the σE envelope stress response, which in turn induces their rapid degradation, thereby promoting cell survival (18, 39, 40). Our results showing that the Bam complex activity can be blocked by a lipoprotein rather than an OMP substrate may provide alternative or additional routes for Bam complex inhibition.

MATERIALS AND METHODS

Bacterial strains and growth conditions. All the bacterial strains used in this study are derived from MC4100 (2) and are listed in Table S2 in the supplemental material. All the strains were constructed by generalized P1 transduction (41). The deletion alleles originated from the Keio collection (42), and the Kan cassettes were excised using the Flp recombinase (43). Strains were grown at either 37°C or 30°C as indicated. Lysogeny broth (LB)-Lennox or minimal glucose medium (26.1 mM Na_2HPO_4, 22 mM KH_2PO_4, 8.5 mM NaCl, 18.6 mM NH_4Cl, 0.2% glucose, 1 mM $MgSO_4$, 100 μg/ml thiamine) was used as a growth medium. A final concentration of 100 μM β-NAD hydrate (Millipore Sigma) was added for the growth of

nadA::Tn*10* and *nadB*::Tn*10* strains. When required, the following concentrations of antibiotics were used: 125 μg/ml ampicillin, 20 μg/ml tetracycline, 25 μg/ml kanamycin, and 20 μg/ml chloramphenicol.

In vivo formaldehyde cross-linking and immunoblot analyses. Cross-linking experiments were performed in at least three biological replicates. Strains were grown in a glucose minimal medium at 30°C to an OD$_{600}$ of 0.7 to 1.2, washed twice in phosphate-buffered saline (PBS) (10 mM Na$_2$HPO$_4$, 1.8 mM KH$_2$PO$_4$, 2.7 mM KCl, 137 mM NaCl, pH 7.6) and normalized to an optical density (OD$_{600}$) of 10 in PBS. Cell suspensions were split into two 200-μl samples; one was subjected to cross-linking, while the second sample was used to determine total levels of OMPs and BamD (see below).

Cross-linking was carried out in 200 μl of cell suspension by addition of formaldehyde to a final concentration of 0.7% for 12 min at room temperature. The reaction was stopped by addition of Tris-Cl (pH 6.8) to a final concentration of 100 mM. The cells of cross-linked and non-cross-linked samples were harvested by centrifugation and resuspended in 100 μl of BBB buffer (1$\times$ BugBuster reagent [Millipore Sigma], 50 mM Tris-Cl, pH 6.8, and 1 μl Benzonase [Millipore Sigma]). After incubation on the bench for 2 to 3 min, 100 μl of 2$\times$ SDS loading buffer was added and samples were heated at 65°C for 15 min.

For immunoblotting, 10 μl of samples, normalized by OD$_{600}$ prior to cross-linking, was separated on SDS-PAGE. The proteins were blotted onto a polyvinylidene difluoride (PVDF) membrane and blocked with 2% nonfat dried milk in wash buffer (1.21 g/liter Tris base, 9 g/liter NaCl, 0.05% Tween 20). The membranes were probed with previously validated polyclonal rabbit antibodies raised against RcsF (1:10,000) (20); BamA (1:40,000) (3); OmpA, OmpC, and OmpF (1:20,000) (44, 45); BamD (1:5,000) (16); and σ70 (1:20,000). σ70 protein was served as a loading control. Donkey anti-rabbit IgG linked to HRP (1:10,000) (GE Healthcare) was used as a secondary antibody. Immunoblots validating band identities using deletions of corresponding nonessential genes are shown in Fig. S7.

The blots were developed with Luminata Crescendo Western HRP substrate (Millipore) and visualized using an ImageQuant LAS 4000 Mini (GE Healthcare). The intensity of BamA and BamAxRcsF bands was quantified using GelQuantNet software. Graphs were built using GraphPad Prism software. Significance analysis was performed using an unpaired *t* test by comparing all strains with the WT (using GraphPad Prism).

SUPPLEMENTAL MATERIAL

Supplemental material for this article may be found at https://doi.org/10.1128/mBio .00660-19.

FIG S1, PDF file, 0.7 MB.
FIG S2, PDF file, 0.7 MB.
FIG S3, PDF file, 0.7 MB.
FIG S4, PDF file, 0.7 MB.
FIG S5, PDF file, 0.7 MB.
FIG S6, PDF file, 0.8 MB.
FIG S7, PDF file, 0.2 MB.
TABLE S1, PDF file, 0.3 MB.
TABLE S2, PDF file, 0.4 MB.

REFERENCES

1. Konovalova A, Kahne DE, Silhavy TJ. 2017. Outer membrane biogenesis. Annu Rev Microbiol 71:539–556. https://doi.org/10.1146/annurev-micro -090816-093754.
2. Malinverni JC, Werner J, Kim S, Sklar JG, Kahne D, Misra R, Silhavy TJ. 2006. YfiO stabilizes the YaeT complex and is essential for outer membrane protein assembly in Escherichia coli. Mol Microbiol 61:151–164. https://doi.org/10.1111/j.1365-2958.2006.05211.x.
3. Wu T, Malinverni J, Ruiz N, Kim S, Silhavy TJ, Kahne D. 2005. Identification of a multicomponent complex required for outer membrane biogenesis in Escherichia coli. Cell 121:235–245. https://doi.org/10.1016/j.cell.2005 .02.015.
4. Lee J, Sutterlin HA, Wzorek JS, Mandler MD, Hagan CL, Grabowicz M, Tomasek D, May MD, Hart EM, Silhavy TJ, Kahne D. 2018. Substrate binding to BamD triggers a conformational change in BamA to control membrane insertion. Proc Natl Acad Sci U S A 115:2359–2364. https:// doi.org/10.1073/pnas.1711727115.
5. Hagan CL, Wzorek JS, Kahne D. 2015. Inhibition of the beta-barrel assembly machine by a peptide that binds BamD. Proc Natl Acad Sci U S A 112:2011–2016. https://doi.org/10.1073/pnas.1415955112.
6. Gessmann D, Chung YH, Danoff EJ, Plummer AM, Sandlin CW, Zaccai NR, Fleming KG. 2014. Outer membrane beta-barrel protein folding is physically controlled by periplasmic lipid head groups and BamA. Proc Natl Acad Sci U S A 111:5878–5883. https://doi.org/10.1073/ pnas.1322473111.
7. Malinverni JC, Silhavy TJ. 2011. Assembly of outer membrane beta-barrel proteins: the Bam complex. EcoSal Plus 4(2). https://doi.org/10.1128/ ecosalplus.4.3.8.
8. Mahoney TF, Ricci DP, Silhavy TJ. 2016. Classifying beta-barrel assembly

substrates by manipulating essential Bam complex members. J Bacteriol 198:1984–1992. https://doi.org/10.1128/JB.00263-16.

9. Schwalm J, Mahoney TF, Soltes GR, Silhavy TJ. 2013. Role for Skp in LptD assembly in Escherichia coli. J Bacteriol 195:3734–3742. https://doi.org/10.1128/JB.00431-13.

10. Charlson ES, Werner JN, Misra R. 2006. Differential effects of yfgL mutation on Escherichia coli outer membrane proteins and lipopolysaccharide. J Bacteriol 188:7186–7194. https://doi.org/10.1128/JB.00571-06.

11. Hagan CL, Kim S, Kahne D. 2010. Reconstitution of outer membrane protein assembly from purified components. Science 328:890–892. https://doi.org/10.1126/science.1188919.

12. Hagan CL, Kahne D. 2011. The reconstituted Escherichia coli Bam complex catalyzes multiple rounds of beta-barrel assembly. Biochemistry 50:7444–7446. https://doi.org/10.1021/bi2010784.

13. Roman-Hernandez G, Peterson JH, Bernstein HD. 2014. Reconstitution of bacterial autotransporter assembly using purified components. Elife 3:e04234. https://doi.org/10.7554/eLife.04234.

14. Rigel NW, Schwalm J, Ricci DP, Silhavy TJ. 2012. BamE modulates the Escherichia coli beta-barrel assembly machine component BamA. J Bacteriol 194:1002–1008. https://doi.org/10.1128/JB.06426-11.

15. Tellez R, Jr, Misra R. 2012. Substitutions in the BamA beta-barrel domain overcome the conditional lethal phenotype of a DeltabamB DeltabamE strain of Escherichia coli. J Bacteriol 194:317–324. https://doi.org/10.1128/JB.06192-11.

16. Sklar JG, Wu T, Gronenberg LS, Malinverni JC, Kahne D, Silhavy TJ. 2007. Lipoprotein SmpA is a component of the YaeT complex that assembles outer membrane proteins in Escherichia coli. Proc Natl Acad Sci U S A 104:6400–6405. https://doi.org/10.1073/pnas.0701579104.

17. Konovalova A, Schwalm JA, Silhavy TJ. 2016. A suppressor mutation that creates a faster and more robust sigmaE envelope stress response. J Bacteriol 198:2345–2351. https://doi.org/10.1128/JB.00340-16.

18. Konovalova A, Grabowicz M, Balibar CJ, Malinverni JC, Painter RE, Riley D, Mann PA, Wang H, Garlisi CG, Sherborne B, Rigel NW, Ricci DP, Black TA, Roemer T, Silhavy TJ, Walker SS. 2018. Inhibitor of intramembrane protease RseP blocks the sigma(E) response causing lethal accumulation of unfolded outer membrane proteins. Proc Natl Acad Sci U S A 115:E6614–E6621. https://doi.org/10.1073/pnas.1806107115.

19. Konovalova A, Perlman DH, Cowles CE, Silhavy TJ. 2014. Transmembrane domain of surface-exposed outer membrane lipoprotein RcsF is threaded through the lumen of beta-barrel proteins. Proc Natl Acad Sci U S A 111:E4350–E4358. https://doi.org/10.1073/pnas.1417138111.

20. Konovalova A, Mitchell AM, Silhavy TJ. 2016. A lipoprotein/beta-barrel complex monitors lipopolysaccharide integrity transducing information across the outer membrane. Elife 5:e15276. https://doi.org/10.7554/eLife.15276.

21. Cano DA, Domínguez-Bernal G, Tierrez A, Garcia-Del Portillo F, Casadesús J. 2002. Regulation of capsule synthesis and cell motility in Salmonella enterica by the essential gene igaA. Genetics 162:1513–1523.

22. Wall E, Majdalani N, Gottesman S. 2018. The complex Rcs regulatory cascade. Annu Rev Microbiol 72:111–139. https://doi.org/10.1146/annurev-micro-090817-062640.

23. Aoki SK, Malinverni JC, Jacoby K, Thomas B, Pamma R, Trinh BN, Remers S, Webb J, Braaten BA, Silhavy TJ, Low DA. 2008. Contact-dependent growth inhibition requires the essential outer membrane protein BamA (YaeT) as the receptor and the inner membrane transport protein AcrB. Mol Microbiol 70:323–340. https://doi.org/10.1111/j.1365-2958.2008.06404.x.

24. Grabowicz M, Silhavy TJ. 2017. Redefining the essential trafficking pathway for outer membrane lipoproteins. Proc Natl Acad Sci U S A 114:4769–4774. https://doi.org/10.1073/pnas.1702248114.

25. Rigel NW, Ricci DP, Silhavy TJ. 2013. Conformation-specific labeling of BamA and suppressor analysis suggest a cyclic mechanism for beta-barrel assembly in Escherichia coli. Proc Natl Acad Sci U S A 110:5151–5156. https://doi.org/10.1073/pnas.1302662110.

26. McCabe AL, Ricci D, Adetunji M, Silhavy TJ. 2017. Conformational changes that coordinate the activity of BamA and BamD allowing beta-barrel assembly. J Bacteriol 199:e00373-17. https://doi.org/10.1128/JB.00373-17.

27. Ricci DP, Hagan CL, Kahne D, Silhavy TJ. 2012. Activation of the Escherichia coli beta-barrel assembly machine (Bam) is required for essential

components to interact properly with substrate. Proc Natl Acad Sci U S A 109:3487–3491. https://doi.org/10.1073/pnas.1201362109.

28. Misra R, Stikeleather R, Gabriele R. 2015. In vivo roles of BamA, BamB and BamD in the biogenesis of BamA, a core protein of the beta-barrel assembly machine of Escherichia coli. J Mol Biol 427:1061–1074. https://doi.org/10.1016/j.jmb.2014.04.021.

29. Hart EM, Gupta M, Wühr M, Silhavy TJ. 2019. The synthetic phenotype of ΔbamB ΔbamE double mutants results from a lethal jamming of the Bam complex by the lipoprotein RcsF. mBio 10:e00662-19. https://doi.org/10.1128/mBio.00662-19.

30. Bakelar J, Buchanan SK, Noinaj N. 2016. The structure of the beta-barrel assembly machinery complex. Science 351:180–186. https://doi.org/10.1126/science.aad3460.

31. Iadanza MG, Higgins AJ, Schiffrin B, Calabrese AN, Brockwell DJ, Ashcroft AE, Radford SE, Ranson NA. 2016. Lateral opening in the intact beta-barrel assembly machinery captured by cryo-EM. Nat Commun 7:12865. https://doi.org/10.1038/ncomms12865.

32. Ruiz N, Gronenberg LS, Kahne D, Silhavy TJ. 2008. Identification of two inner-membrane proteins required for the transport of lipopolysaccharide to the outer membrane of Escherichia coli. Proc Natl Acad Sci U S A 105:5537–5542. https://doi.org/10.1073/pnas.0801196105.

33. Chng SS, Ruiz N, Chimalakonda G, Silhavy TJ, Kahne D. 2010. Characterization of the two-protein complex in Escherichia coli responsible for lipopolysaccharide assembly at the outer membrane. Proc Natl Acad Sci U S A 107:5363–5368. https://doi.org/10.1073/pnas.0912872107.

34. Qiao S, Luo Q, Zhao Y, Zhang XC, Huang Y. 2014. Structural basis for lipopolysaccharide insertion in the bacterial outer membrane. Nature 511:108–111.

35. Dong H, Xiang Q, Gu Y, Wang Z, Paterson NG, Stansfeld PJ, He C, Zhang Y, Wang W, Dong C. 2014. Structural basis for outer membrane lipopolysaccharide insertion. Nature 511:52–56.

36. Sutterlin HA, Malinverni JC, Lee SH, Balibar CJ, Roemer T. 2017. Antibacterial new target discovery: sentinel examples, strategies, and surveying success, p 1–29. In Fisher JF, Mobashery S, Miller MJ (ed), Antibacterials. Topics in medicinal chemistry, vol 25. Springer, Cham, Switzerland.

37. Storek KM, Auerbach MR, Shi H, Garcia NK, Sun D, Nickerson NN, Vij R, Lin Z, Chiang N, Schneider K, Wecksler AT, Skippington E, Nakamura G, Seshasayee D, Koerber JT, Payandeh J, Smith PA, Rutherford ST. 2018. Monoclonal antibody targeting the beta-barrel assembly machine of Escherichia coli is bactericidal. Proc Natl Acad Sci U S A 115:3692–3697. https://doi.org/10.1073/pnas.1800043115.

38. Ieva R. 2017. Interfering with outer membrane biogenesis to fight Gram-negative bacterial pathogens. Virulence 8:1049–1052. https://doi.org/10.1080/21505594.2017.1296617.

39. Walsh NP, Alba BM, Bose B, Gross CA, Sauer RT. 2003. OMP peptide signals initiate the envelope-stress response by activating DegS protease via relief of inhibition mediated by its PDZ domain. Cell 113:61–71. https://doi.org/10.1016/S0092-8674(03)00203-4.

40. Mecsas J, Rouviere PE, Erickson JW, Donohue TJ, Gross CA. 1993. The activity of sigma E, an Escherichia coli heat-inducible sigma-factor, is modulated by expression of outer membrane proteins. Genes Dev 7:2618–2628. https://doi.org/10.1101/gad.7.12b.2618.

41. Silhavy TJ, Berman ML, Enquist LW (ed). 1984. Experiments with gene fusions. Cold Spring Harbor Laboratory, Cold Spring Harbor, NY.

42. Baba T, Ara T, Hasegawa M, Takai Y, Okumura Y, Baba M, Datsenko KA, Tomita M, Wanner BL, Mori H. 2006. Construction of Escherichia coli K-12 in-frame, single-gene knockout mutants: the Keio collection. Mol Syst Biol 2:2006.0008. https://doi.org/10.1038/msb4100050.

43. Datsenko KA, Wanner BL. 2000. One-step inactivation of chromosomal genes in Escherichia coli K-12 using PCR products. Proc Natl Acad Sci U S A 97:6640–6645. https://doi.org/10.1073/pnas.120163297.

44. Misra R, Reeves PR. 1987. Role of micF in the tolC-mediated regulation of OmpF, a major outer membrane protein of Escherichia coli K-12. J Bacteriol 169:4722–4730. https://doi.org/10.1128/jb.169.10.4722-4730.1987.

45. Zimmermann R, Wickner W. 1983. Energetics and intermediates of the assembly of protein OmpA into the outer membrane of Escherichia coli. J Biol Chem 258:3920–3925.

46. Ruiz N, Falcone B, Kahne D, Silhavy TJ. 2005. Chemical conditionality: a genetic strategy to probe organelle assembly. Cell 121:307–317. https://doi.org/10.1016/j.cell.2005.02.014.